Behaviour of Ultra-Thin Continuously Reinforced Concrete Pavements under moving axle loads

Concrete pavements are normally deemed to be rigid pavements that are designed using design principles based on the beam on elastic support equations as derived by Westergaard in 1926. In the recent past, Ultra-Thin Continuously Reinforced Concrete Pavements (UTCRCP) have been constructed with concrete layers as thin as 40mm. These pavements have been subjected to millions of load cycles without any noticeable permanent damage. The design of these flexible concrete pavements has proven to be problematic as they are neither rigid nor truly flexible. To improve understanding of the soil-structure interaction that occurs when wheel loads move over the UTCRCP, it was decided to use a geotechnical centrifuge to test UTCRCP scale models at 10G. The test results confirm that the centrifugal forces have a significant effect on the stiffness of the scaled pavement system. The interaction between the supporting layers and the thin, flexible reinforced concrete layer could be observed and it is clear that the behaviour of this type of pavement under moving axle loads differs notably from the assumed behaviour for both rigid and flexible pavements. Experimental results indicate that designers should not only consider the loading pattern caused by interaction between wheels on an axle and different axles, but also the rutting of supporting layers that requires the reinforced concrete surface layer to not only span across gaps below the surface, but also resist increased vertical pressure between wheel paths.

Keywords: concrete pavement design, ultra-thin concrete pavement, centrifuge modelling, cemented bases, UTCRCP

Subject classification codes: include these here if the journal requires them

Introduction

Ultra-Thin Continuously Reinforced Concrete Pavement (UTCRCP) consists of a 40 to 55 mm thick layer of high strength concrete (with uniaxial compressive strengths in the region of 90 MPa), containing approximately 80 kg/m^3 of steel fibre, as well as a steel mesh of 5.6 mm high yield reinforcing bars spaced at about 50 mm centre to centre in both the longitudinal and transverse directions of the pavement. The use of UTCRCP can

result in a significant saving in the volume of material required for a pavement designed to accommodate a given traffic load.

As part of the South African National Highway Renewal Programme, test sections of UTCRCP have been constructed. The test sections were subjected to Heavy Vehicle Simulator (HVS) testing with wheel loads more than double the expected traffic loads, without any noticeable permanent damage (Kannemeyer *et al.* 2007). To induce failure water had to be introduced to the pavement to promote pumping.

Kannemeyer *et al.* (2007) noted that debonding occurred between the ultra-thin concrete layer and the supporting layer directly underneath is. It was hypothesised that the cause of the debonding was pumping of the substructure materials. Denneman (2011) summarised that damage propagation in UTCRCP observed during HVS testing consisted of fines pumping through transverse shrinkage cracks when water was added. The pumping resulted in loss of support at shrinkage cracks. This resulted in an increase in bending stresses and secondary cracks forming approximately 300 mm from the original cracks, in the longitudinal direction. Both these statements are related to damage propagation and failure of UTCRCP caused by a loss of support due to pumping.

The fact that the HVS consists of a single wheel load, causing a load set to be much higher than the actual load that the pavement would experience repeatedly, leaves a gap in the understanding of the actual behaviour of UTCRCP under repeated rolling axle loads. Only by understanding the failure mechanisms of UTCTCP can design assumptions be refined to limit the risk of UTCRCP failing under repeated moving axle loads.

The focus of this research is thus to improve understanding of the response of UTCRCP to traffic loading, by identifying potential failure mechanisms of UTCRCP unrelated to loss of support due to pumping.

Background

Conventionally, there are two types of pavement, flexible pavements and rigid pavements. Typically, concrete pavements are deemed to be rigid pavements and asphalt pavements are deemed to be flexible pavements. Figure 1 shows the profile of typical asphalt and concrete pavements. The uppermost layer is usually a bound layer of asphalt or concrete. The concrete layer of rigid pavements is structurally dominant and the materials of the supporting layer do not need to have such a high quality (Huang 1993). The asphalt layer is not as structurally dominant as concrete. The typical design approach for flexible pavements is that stress exerted on the surface is spread gradually with depth through layers of materials that become weaker further from the surface.

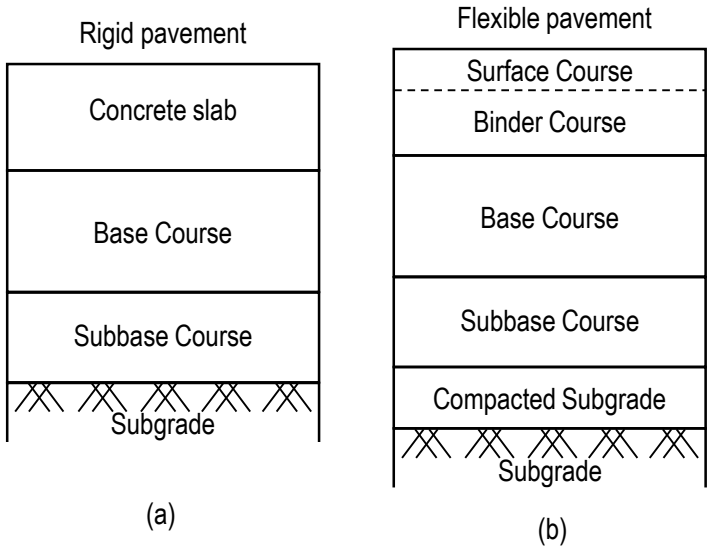

Figure 1 Typical cross section of (a) rigid pavement and (b) flexible pavement (adapted from Huang (1993))

Rigid pavements, or conventional concrete pavements, are designed for fatigue cracking of the concrete layer. To determine critical stresses, three load cases of thick rectangular concrete panels are considered (Westergaard 1926). For the first load case, the load is located at a corner of the panel and the tensile stress at the top of the panel is considered. For the second load case, the load is located in the centre of the panel and the tensile stress at the bottom of the panel is considered. For the third load case, the load is

located on the edge, a considerable distance away from the corners. The tensile stress at the bottom of the panel is considered.

The radius of relative stiffness is a characteristic length of a pavement system. It is used in analytical solutions to determine stresses in concrete pavements. The radius of relative stiffness, denoted by l_k, for systems that use spring foundations is defined by Equation 1:

$$l_k = \sqrt[4]{\frac{E_c h^3}{12(1-{\nu_c}^2)k}} \qquad \textit{Equation 1}$$

Where the stiffness properties of the concrete slab are the material stiffness (Young's Modulus), E_C, and Poisson's Ratio, ν_c, and the thickness, h. The stiffness of the supporting layer is quantified by the modulus of subgrade reaction, k. The modulus of subgrade reaction is determined using a plate bearing test. The modulus of subgrade reaction can also be back-calculated from the deflected shape of pavements (Bowles 1996).

The radius of relative stiffness for rigid pavements for rigid pavements calculated by Westergaard (1926) ranged from 430 mm to 1385 mm and it was stated that the typical value is 914 mm. It has also been stated that the radius of relative stiffness should fall between 570 mm and 2032 mm, where the lower limit is selected considering that pavement systems with lower radius of relative stiffness values cannot be modelled adequately using a slab-on-grade model (ARA and Division 2004, Gerber 2011).

The concrete layer of UTCRCP is less than 20% of the thickness of conventional concrete pavements. This leads to the question of whether UTCRCP should rather be designed as a flexible pavement. Flexible pavements normally consist of compacted layers, sealed by a thin bituminous or asphalt layer. These pavements are designed by considering fatigue cracking of the asphalt layer and rutting of the entire pavement

profile. The most critical strains occur under or near the load and the tensile strain at the bottom of the surface layer and the compressive strain at the top of the subgrade are considered for design. When arrangements of wheels are considered in analysis, superposition is used.

Stress distribution caused by load configuration

The vertical stress caused by multiple wheel loads do not interact at shallow depths. At greater depths, the vertical stress distributions start overlapping and the pavement material that is situated at this depth is subjected to a higher stress between the two wheels of a tandem axle than if no superposition is taken into account. If the behaviour of the substructure is investigated, overlapping stress fields of wheel loads, as indicated in Figure 2, become important.

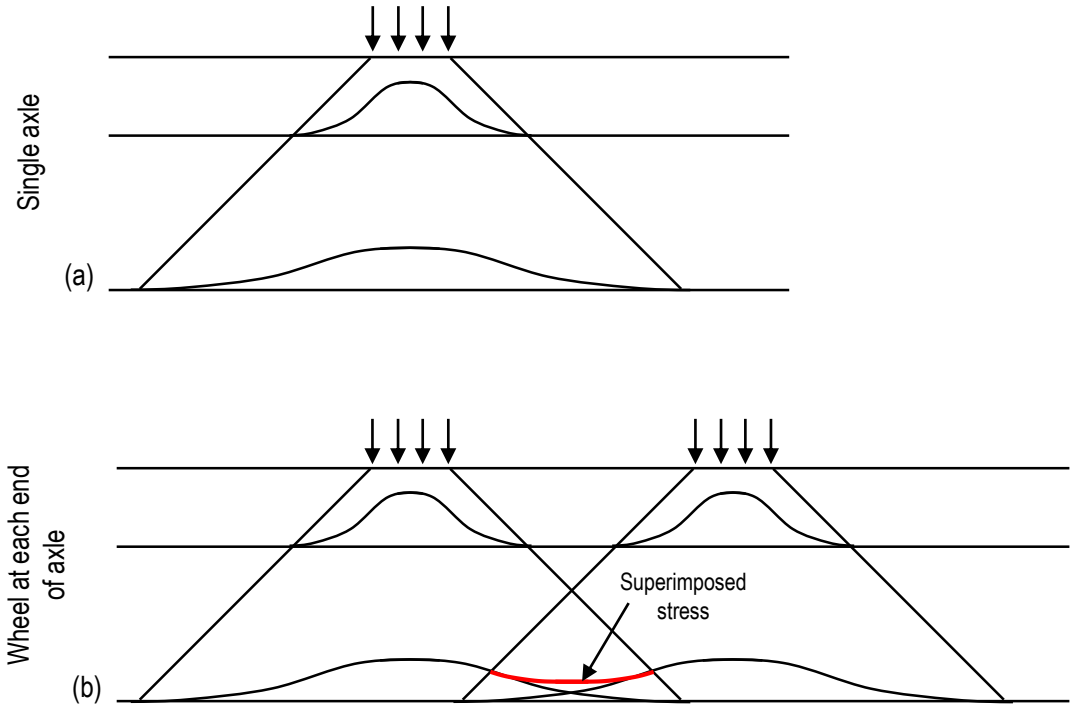

Figure 2 Vertical stress distribution of (a) single wheel and (b) axle loads (adapted from Kim (2007))

The distance between the wheel arrangements at the ends of an axle is approximately 1980 m (Huang 1993). It is anticipated that the vertical stress distributions of the wheel loads from the axle ends overlap and interact from a certain depth. If it is assumed that the load spreading in all pavement layers happened at 45º, the depth at which the vertical stress distributions caused by two point loads placed an axle length apart (1980 mm), would overlap would be 990 mm. The overlap depth will reduce if the load is applied over an area. Additionally, it is known that load spreading is dependent on the layer material properties and can occur at angles greater than 45º (Mones Ruiz *et al.* 2019).

This stress overlap and interaction are often ignored during conventional flexible and rigid pavement design procedures. The alternative nature of UTCRCP, with a very thin high strength steel fibre reinforced concrete layer, leads to the proposal that the interaction between the wheel arrangements at the ends of an axle should be considered in the design process.

Scaled modelling of pavements

The response of UTCRCP to traffic loading can be investigated more thoroughly using scaled physical modelling, as full-scale testing is expensive. The nonlinear behaviour and shear strength of unbound base and subgrade materials are dependent on the effective stress conditions of the pavement structure. The vertical effective stress is dependent on the weight above the layer in question and the water table position, while the vertical effective stress and the coefficient of lateral earth pressure at-rest are used to determine the horizontal effective stress. Scaled modelling results in a reduced depth and vertical effective stress which influences the reliability of the model response.

However, scaled testing has been done on pavements with some success (Van de Ven and De Fortier Smit 2000, Martin *et al.* 2003, Bueno *et al.* 2016, Bowman and Haigh

2019). Scaling factors of 1:10 and 1:3 have been used. It was commented that pavement models that were one tenth the size of full scale posed practical difficulties such as constructing very thin pavement layers (Van de Ven and De Fortier Smit 2000). Martin *et al.* (2003) showed that comparable stress distributions existed for simple pavement structures when a scaling factor of 3 was used and that rutting could be predicted. They recommended that factors such as the nonlinear behaviour of unbound base and subgrade materials, and shear stresses affect deformation in pavements. These factors are dependent on the effective stress conditions of the pavement structure.

In geotechnical engineering, centrifugal acceleration is used to raise the stress in the scaled model to that of a full-scale prototype. Geotechnical centrifuges are used for this purpose. Recently there has been a move toward scaled physical modelling of pavements in conjunction with a geotechnical centrifuge (Kearsley *et al.* 2014, Bayton *et al.* 2018, Dave and Dasaka 2018, Lukiantchuki *et al.* 2018, Saboya *et al.* 2020, Smit and Kearsley 2022). Various model configurations with scaling factors ranging from 10 to 30 have been constructed and tested successfully. Kearsley *et al.* (2014) successfully designed a scaled concrete mix of which the load-deformation behaviour replicated that of full-scale high strength steel fibre reinforced concrete.

Centrifuge modelling of UTCRCP

Smit and Kearsley (2022) used centrifuge modelling to do a conceptual investigation of the response of Ultra-Thin High Strength Steel Fibre Reinforced Concrete pavement to traffic loading. Three main observations were made during the investigation:

- the concrete layer detached from the substructure forming a void when the pavement was unloaded,

- the cement stabilized base may have cracked discretely and caused stress concentrations in adjacent layers, and
- the complex load configurations resulted in the maximum vertical strain in the substructure not being in the wheel path at depth.

The applicability of these observations and how they should influence the design of UTCRCP is however questionable, as the models were simplified to two- and three-layer pavement systems using dry sand and cement stabilised sand to represent the granular materials. The total depth of the models was 300 mm of dry sand, which would represent a 3 m fill at full scale. Additionally, the significance of the effect of centrifugal acceleration on the pavement response was not verified.

The purpose of this study was to investigate the response of UTCRCP to traffic loading using a multilayer pavement system and a more complex load application setup. The aims discussed in this paper are:

- Evaluating the significance of the effect of centrifugal acceleration on the pavement response
- Establishing whether scaled models containing representative granular materials can be built with scaled layer thicknesses of 1:10 to provide qualitative behavioural mechanisms similar to prototype multi-layer pavement systems.
- Determining qualitative behavioural mechanisms for scaled layered UTCRCP under moving axle loads.

Experimental methodology

The behaviour of UTCRCP under traffic loading was modelled by constructing scaled models at one tenth of the size of actual pavements and conducting tests at 10G in the

geotechnical centrifuge.

Scaling rules were followed to not only ensure realistic axle loads and wheel surface contact areas, but also result in spreading of loads through the pavement layers. In the first part of the experiment, the effect of the centrifugal forces on the individual pavement layers as well as the layered pavement system was established by doing scaled plate bearing tests. In the second part of the experiment a section of UTCRCP was constructed and subjected to rolling wheel loads, with a wheel contact pressure of 550 kPa, while under 10G acceleration.

Model configuration

Both the plate bearing and the rolling wheel tests were conducted on pavement layers. Using a scaling factor of 10, the selected, subbase and base layers that would typically be 150 mm thick where compacted in 15 mm thick layers, while the 90 MPa reinforced concrete surface layer was cast to be 5 mm thick. The concrete layer was reinforced with a 0.5 mm thick steel wire mesh, with wires spaced at 5 mm in both directions. To ensure that the pavement layer did not rest directly on the steel base plate a 30 mm thick compacted subgrade layer was placed below the selected subgrade.

Plate bearing tests were conducted at 1G and 10 G for individual 15 mm thick compacted layers as illustrated in Figure 3 (a), the pavement system without the concrete surface layer as indicated in Figure 3 (b) and the complete pavement system as indicated in Figure 3 (c). A rolling wheel load test was conducted on the complete pavement system indicated in Figure 3 (c).

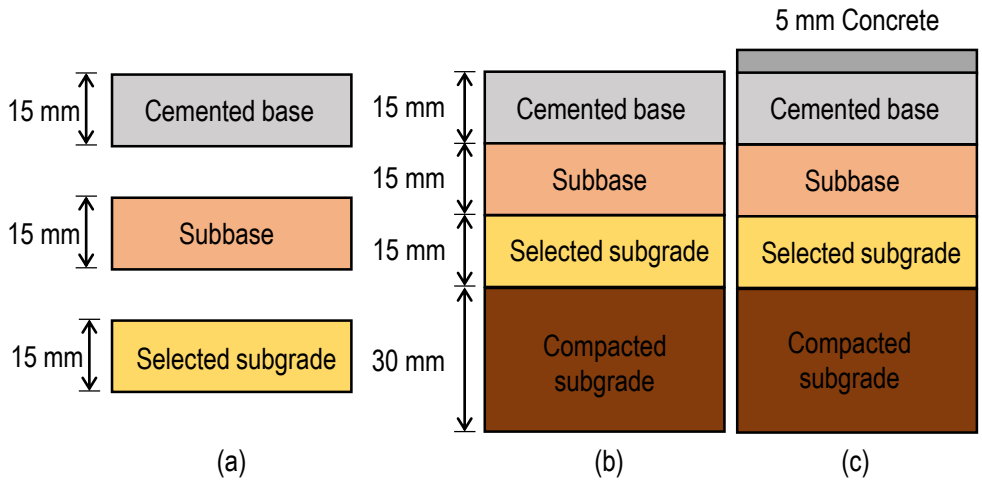

Figure 3 Layer systems and layers tested a) individual layers, b) base top layer system and c) concrete top layer system

Model preparation

The pavement layers were constructed using materials obtained from an UTCRCP test site. The materials were scaled by crushing and screening the coarse material, that had a maximum particle size of 26.3 mm, to ensure that the scale model material had a maximum particle size of 2.63 mm. The volume of coarse material that was retained on the 2.63 mm sieve was replaced with silica sand to ensure that layers would be compactable. The base layer was stabilized using 2.5% cement. The properties of each of the pavement layers can be seen in Table 1. The optimum moisture content and maximum density of each material was determined to calculate the required layer density, based on the typical percentage compaction required for the layer. For each layer, the required mass of material was calculated using the relevant layer volume and selected layer density. The required mass was compacted to form the relevant volume. Manual compaction was used as seen in Figure 4.

Table 1: Pavement layer properties.

Layer	Moisture content (%)	Density (kg/m^3)	Compaction (%)
Cemented base	4.53	2 127	97

Subbase	4.53	2 079	95
Selected	7.64	2 140	93
Compacted subgrade	7.72	2 059	90

Figure 4: Manual compaction of layers.

Testing setup & procedure

Plate bearing test

The load-displacement behaviour, ultimate bearing capacity and the modulus of subgrade reaction were determined using the plate bearing test. Scaled plate bearing tests of the respective materials, as well as of two pavement systems, were conducted. The first pavement system consisted of all the layers up to the base layer, and the second system consisted of the complete pavement, i.e. up to the concrete layer.

Figure 5 (a) and (b) show that the scaled material layers tested individually each had a 15 mm thickness and 150 mm radius. The layers were placed on a stiff plate and confined by circular constraint. A vertical load was applied over a circular area with a 30 mm diameter. The average displacement recorded from three Linear Variable Displacement Transducers (LVDTs) was used to determine the vertical displacement of the loaded area, while a load cell was used to record the load applied. Figure 5 (c) shows

that radius of each layer in the pavement systems reduced from the bottom layer to the surface layer. It also illustrates how the layers were constrained. Figure 6 shows the plate bearing test setup as used in the centrifuge, as well as the construction quality of the models.

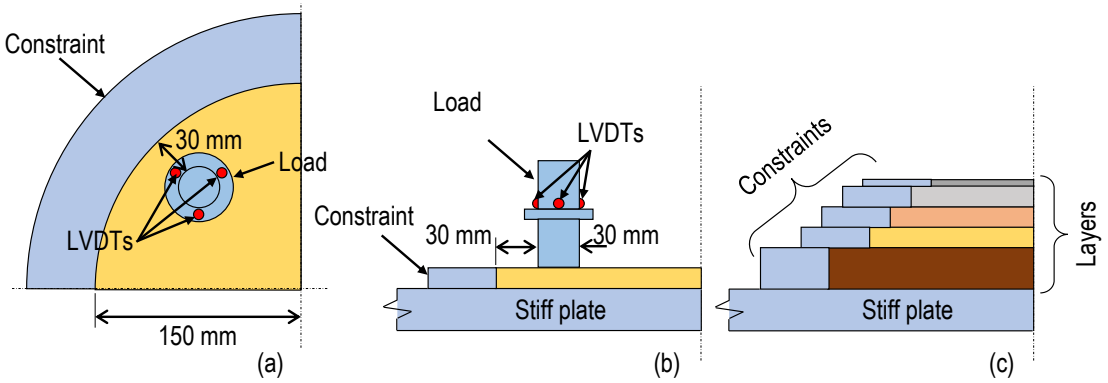

Figure 5 Plate bearing test setup in (a) plan view and (b) side view of single layer, as well as (c) side view of multilayer system

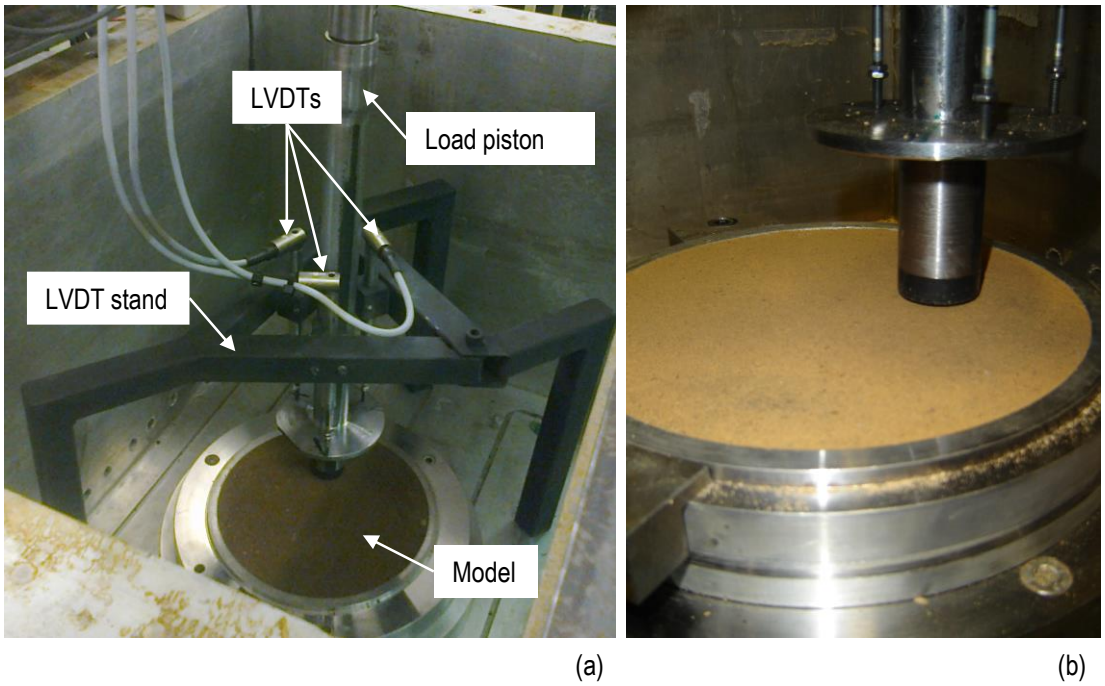

Figure 6 Plate bearing (a) test setup and (b) close-up illustrating construction quality

Rolling wheel load test

Figure 7 (a) shows the plan layout of the 800 mm by 300 mm concrete pavement surface as well as the elevation view of the model. Similar to the plate bearing test pavement

systems, the area of the pavement layer reduced from the bottom to the surface and the layers were confined using steel constraints.

The wheel load applied during testing was based on an Equivalent Standard Axle Load (ESAL) of 80 kN applied to an axle with a single wheel at each end. At full scale, the contact area of each wheel is 330 mm long and 220 mm wide, resulting in a vertical contact pressure of 550 kPa on the road surface. For a typical truck, the wheels on the axle would be 1980 mm apart. The wheel contact area of the scaled model was 33 mm by 22 mm and the wheel spacing was 198 mm. Two axles were modelled to compare the effect of the interaction of load in the transverse and longitudinal direction. The two axles were spaced 200 mm apart, forming a loading cart on which weights were placed to simulate the required load. The loading was quasi-static, with an average rolling speed of 16.7 mm/s (which is approximately 6 km/hr at prototype scale). A screw motor was used to move the loading cart.

The pavement response was measured using a total of eight LVDTs that were built into the layers. Four LVDTs were placed in the wheel centreline and four LVDTs were placed in the axle centreline. The LVDTs were placed at the layer interfaces, for example, between the concrete layer and base layer. The vertical displacement of each LVDT was recorded at 50 Hz. Figure 8 (a) shows the LVDTs and their locations with respect to the pavement layers and Figure 8 (b) shows the loading cart and the screw feed motor.

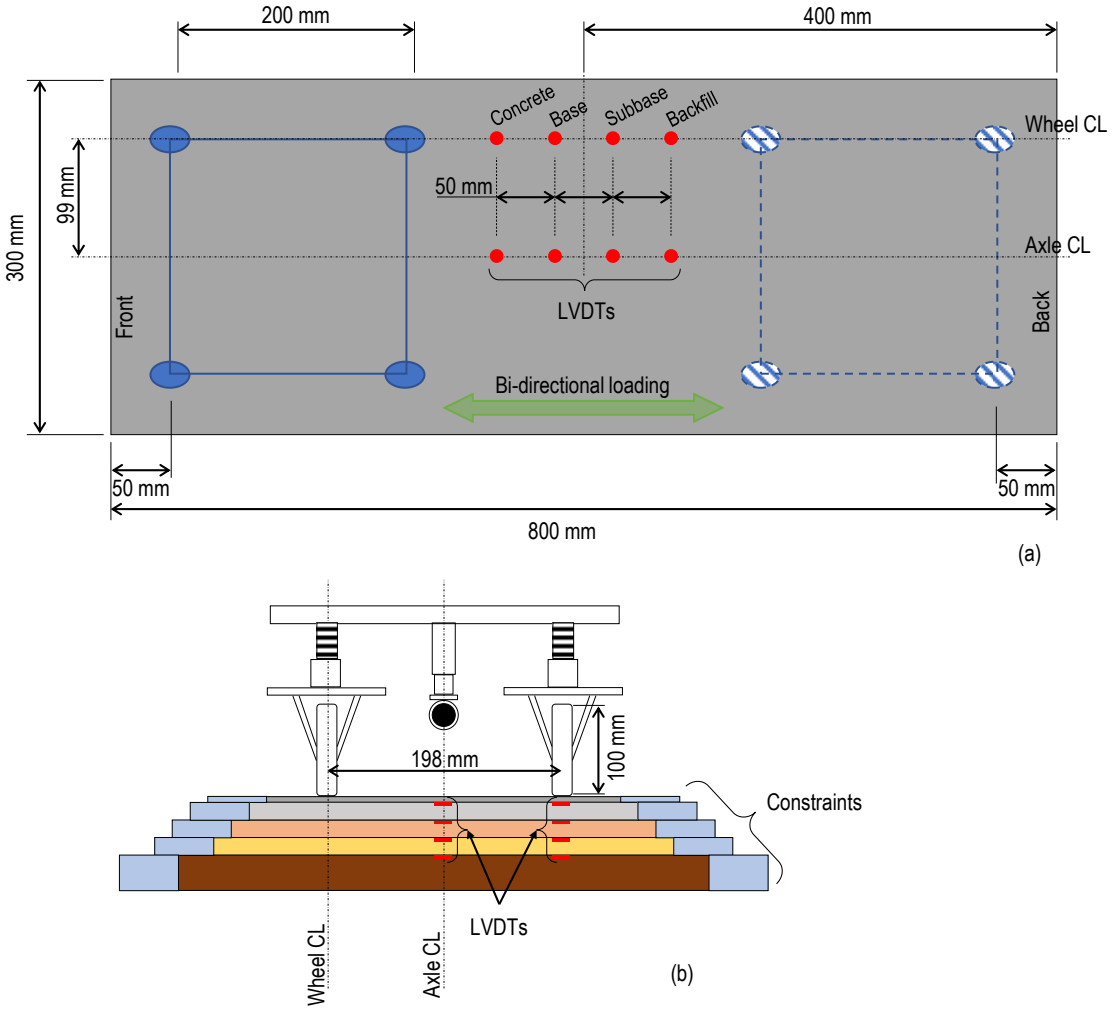

Figure 7 Model setup of the traffic loading model in a) plan view and b) elevation view

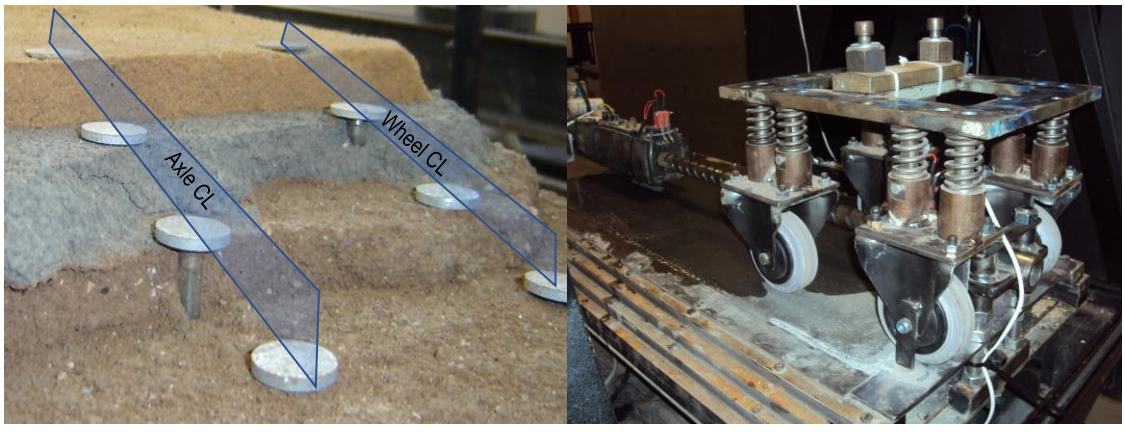

Figure 8 Testing setup with a) the LVDT locations and b) load application setup

Results & discussion

Load-deflection behaviour

The plate bearing test was conducted to determine the effect of the gravitational acceleration on the stiffness and bearing strength of the material layers and pavement systems. The effect of seating during the plate bearing test was deliberately not removed to ensure that all the trends can be seen. Figure 9 (a) show the load-deflection behaviour of the individual materials at 1G and 10G, while Figure 9 (b) show the load-deflection behaviour of the pavement systems at 1G and 10G.

Figure 9 (a) indicates the brittle failure mechanism of the cement stabilised base layer and it can be concluded that the failure of this layer is not affected by the increased confinement provided by the centrifugal forces (1G versus 10G). These results indicate that scaled cement stabilised pavement layers tested at 1G in normal laboratory conditions, would have the same strength and stiffness than the full-scale equivalent. Both the strength and the stiffness of the selected and subbase soil layers are however notably affected by confinement. These results indicate that even for relatively small layer thicknesses, the lack of confinement resulting from scaled material layers, would cause premature failure of layerworks. Figure 9 show the seating effect to complete failure of the respective models. If the stress-displacement from after the seating effect up to the stress of a typical wheel pressure (approximately 550 kPa) is considered, the trends of the individual soil layers are approximately linear. This indicates that the constructed soil layer would sustain repeated standard axle wheel loads without fast deterioration.

In Figure 9 (b), the behaviour of two pavement systems modelled is shown. The load-deflection behaviour shows that both pavement systems were affected by the gravitational acceleration. It was thus decided that scaled pavements should be tested in the centrifuge to ensure realistic behaviour of the supporting soil layers. Although the

strength and stiffness of the cement stabilised layer is not affected by gravitational forces, all the layers in the pavement should be included in the model, as the relative stiffness of the supporting layers affect the behaviour of the subbase.

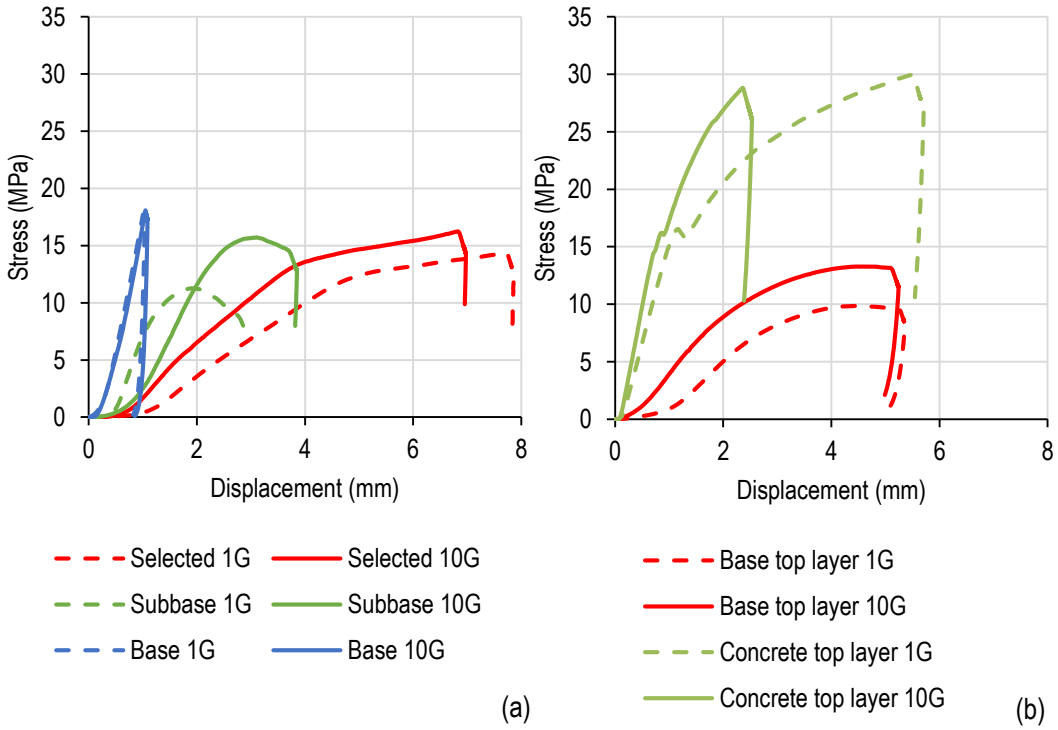

Figure 9 Stress-displacement behaviour of a) scaled single material layers and b) scaled multi material layer systems at 1G and 10G

The load carrying capacity of the scaled pavements as indicated in Figure 9 (b) is an order of magnitude higher than the load that can be exerted by the wheels of vehicles using pneumatic tyres. As the loads that the concrete surface layer should experience under traffic is not supposed to exceed 550 kPa, the load-deflection behaviour of the pavement in this load range can be seen in Figure 10. The relative linearity of the concrete surface graphs in this figure again indicates that scale model should be able to resist repeated wheel loads without significant permanent damage when considering the load-deflection behaviour at loads in the range of 550 kPa. Although the concrete top layer model at 1G deflects only marginally more than at 10G, the base top layer model behaviour seems to be notably affected by the gravitational forces. This confirms that even at relatively small loads scaling could result in distorted behaviour of layered soil systems.

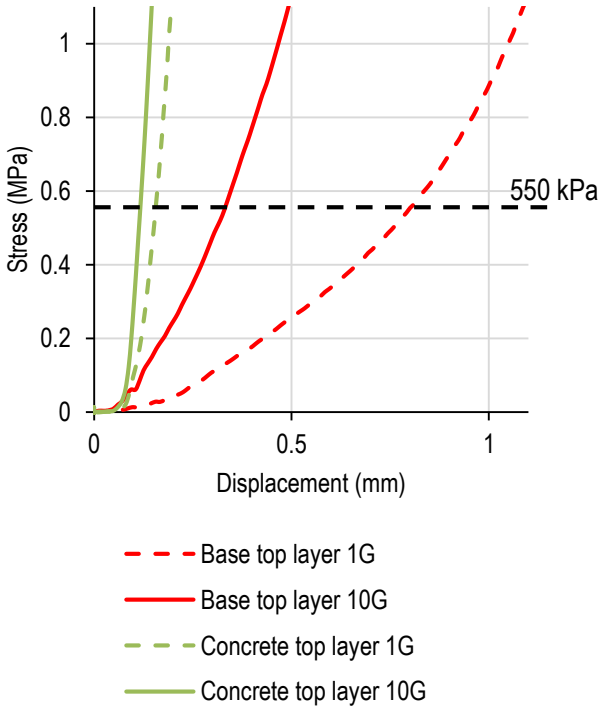

Figure 10 Stiffness of scaled multi material layer systems at 1G and 10G

The modulus of subgrade reaction for each layer was determined using the slope of the applied pressure deflection line of the layered system tested at 10G, for a pressure change from 200 kPa to 550 kPa. After a scaling factor of 10 was applied to the layer thickness, k-values were calculated as indicated in Table 2. Typical modulus of subgrade reaction values range from about 15 kPa/mm for fine grained soils with a presumed bearing capacity in the region of 100 kPa to more than 80 kPa/mm for coarse, clean gravel with a presumed bearing capacity in the region of 500 kPa (Marais and Perrie 1993). Where cement stabilized subbase layers are used, design k-values up to 245 kPa/mm can be used (Marais and Perrie 1993). The modulus of subgrade reaction values obtained from the scaled models are high, but in the same order of magnitude as that reported in literature for actual pavement layers.

Table 2: Modulus of subgrade reaction stiffnesses

Layer	10G system stiffness (kPa/mm)
Cemented base	230
Sub-base	162

Selected subgrade	101
Compacted subgrade	274

Traffic loading of scaled model

Displacement versus time

The measured displacement of each layer as a function of time can be seen in Figure 11 for the sensors in the wheel centreline. These results indicate that significant permanent deformation took place the first time the axle moved over the pavement. For each subsequent load cycle there was a fairly constant reversible vertical displacement, while the increase in permanent vertical displacement decreased with increased load cycles.

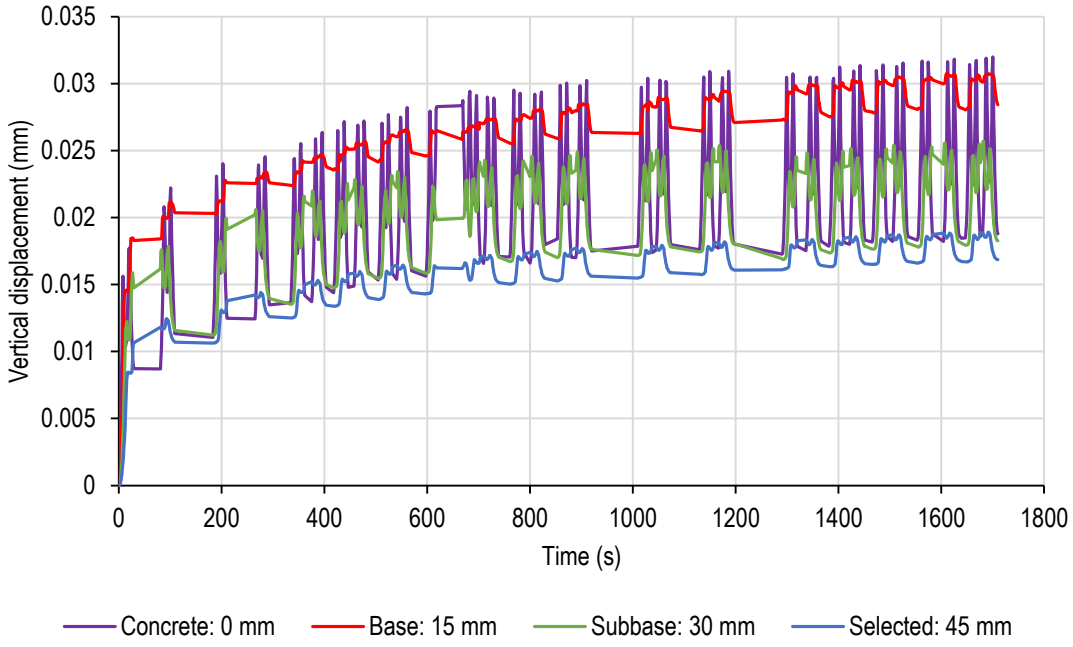

Figure 11 Displacement vs time under the concrete, base, subbase and selected layers in the wheel CL

The vertical displacement of the individual layers are more visible when only the first eight axle load cycles are considered as in Figure 12. The load was applied by a loading cart with two axles that moved bi-directionally over the pavement, while the vertical movement of the different layers was recorded using LVDTs that were placed 50 mm

apart. When the loading cart moved forward, it reached the measurement point under the concrete layer first, but when it moved backwards, the measuring point under the concrete layer was reached last. In Figure 12 the point A1 was reached when the front axle of the loading cart reached the position of the LVDT under the concrete layer, when moving forward for bi-directional loop A. Points A2 and A3 were recorded when the back axle of the loading cart reached the concrete layer measurement point on the forward (point A2) and backward (point A3) section of loop A respectively, while point A4 indicates the moment when the front axle reached the concrete layer measurement point on the backwards moving section of loop A. The same pattern of loading can be seen for bi-directional loop B.

For the purposes of this discussion, each layer was considered to be unloaded approximately 125 mm or 7.5 seconds before the first peak of each bi-directional loop. Similarly, each layer was fully loaded when the first peak of each bi-directional loop was reached.

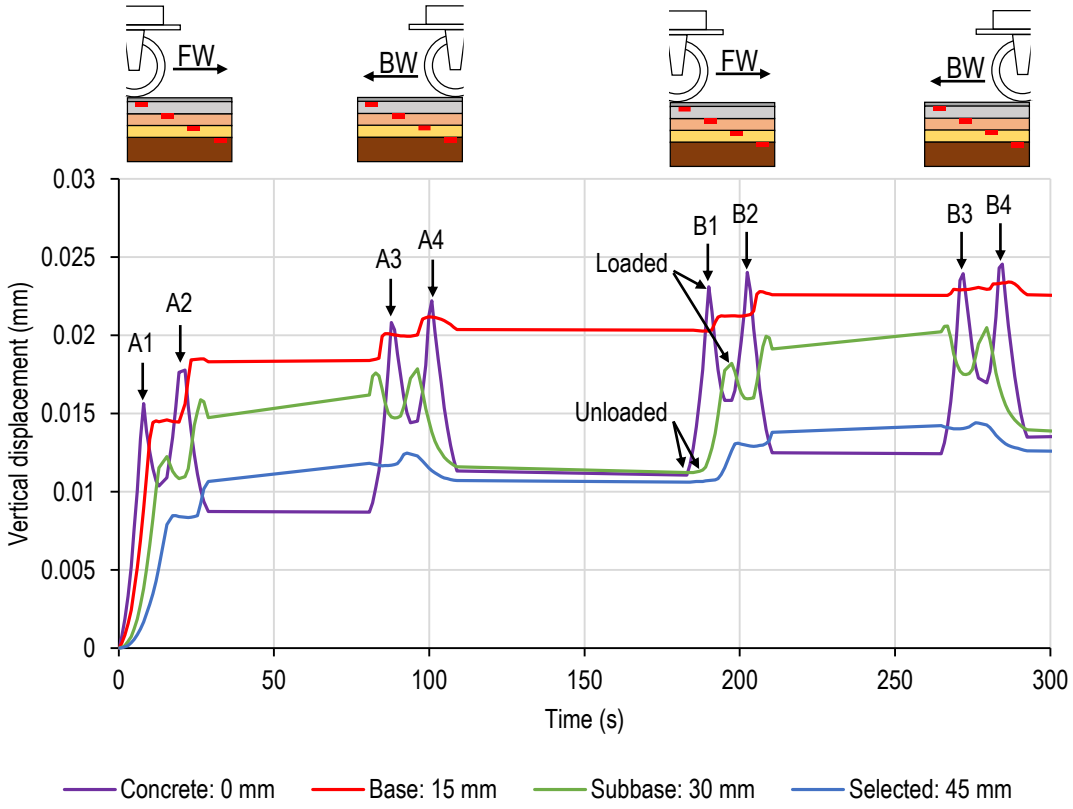

Figure 12 Displacement vs time of the first eight load cycles

The vertical displacement of the concrete layer indicates the effect of the eight separate deflection peaks caused by the eight load cycles. Although the distance between the front and the back axle was selected to be the same as the distance between the wheel paths of the axle, it is clear that this distance is small enough for the concrete pavement to experience a load effect between the two axles. It is only when the whole cart moved away, that the vertical deformation returned to a vertical displacement value that can be considered to be the permanent vertical displacement for an unloaded pavement. The concrete layer seems to be in the unloaded condition when the loading cart is at either end of the pavement.

In contrast, the subbase and the selected layer are still feeling the effect of the loading cart when it was parked at the back end of the pavement, before it commences with the backwards rolling of the bi-directional loop. The influence zone of a wheel load

on UTCRCP is thus notably larger than expected or assumed during any conventional pavement design procedure. These results indicate that single point loads cannot be used to design UTCRCP and heavy vehicle simulators that use single wheels would not adequately reflect the behaviour of these pavements under axle loads.

It is also interesting to note that the stabilized base layer only showed behaviour similar to the other layers up to the peak of the first load cycle, where after limited vertical displacement was observed. These results indicate that significant permanent damage occurred during the first load cycle. As the permanent vertical displacement of the stabilized base layer exceeded that of the concrete layer, the results indicate that permanent rutting took place in the wheel path, directly under the concrete layer. As the concrete layer is highly reinforced with steel, it, in contrast to the base layer, had sufficient ductility to return to a less deflected state.

The fact that the peak vertical deformations for the different layers were reached at different points in time, makes it difficult to compare the behaviour of the different layers. By assuming the loading cart was moving at a constant speed of 16.7 mm/s (which equates to approximately 6 km/hr at prototype scale), it is possible to plot deflection bowls as a function of distance from the measurement point for the different pavement layers.

Deflection bowls

The deflection bowl, as measured when the loading cart approached the measurement points for the first load cycle, can be seen in Figure 13 for all the pavement layers in the wheel path and the axle centreline. These deflections were calculated relative to the point at rest before loading started. As expected, the deflection in the wheel path (WP) decreases with increased depth below the surface. The concrete layer moved down in the axle centreline (CL), resulting in some membrane action, pushing the soil layers down.

This confinement, would result in the soil layers placing upward pressure on the thin concrete layer, causing it to bend upwards (or hog) and possibly resulting in longitudinal lengthwise cracks opening up, if the concrete layer is not sufficiently reinforced in the width of the pavement to resist this pressure. Between the wheel paths, the deflection of all the pavement layers were similar.

To determine whether the thin concrete layer deteriorated as more load cycles were applied, the deflection bowl of the concrete pavement can be compared for different load cycles, as seen in Figure 14. These results indicate that slightly more deflection was recorded in the wheel path under the concrete layer, for the first wheel load cycle than for any subsequent load cycle. The deflection bowl does however indicate resilient behaviour with no noticeable change in the load deflection behaviour of the concrete layer taking place in sixty load cycles.

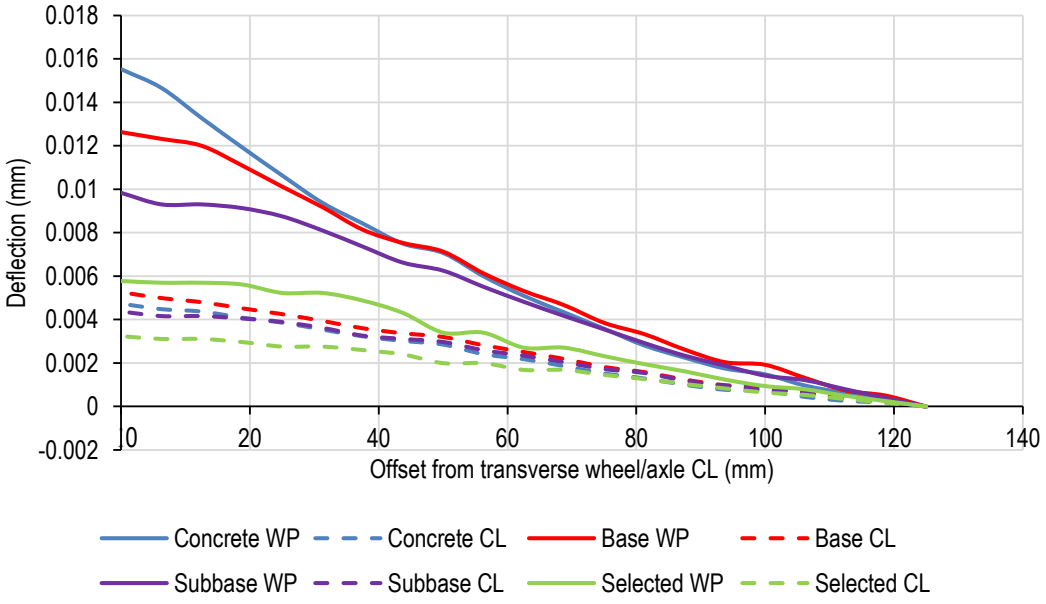

Figure 13 Deflection bowls of all layers for the first load cycle relative to the point at rest before loading

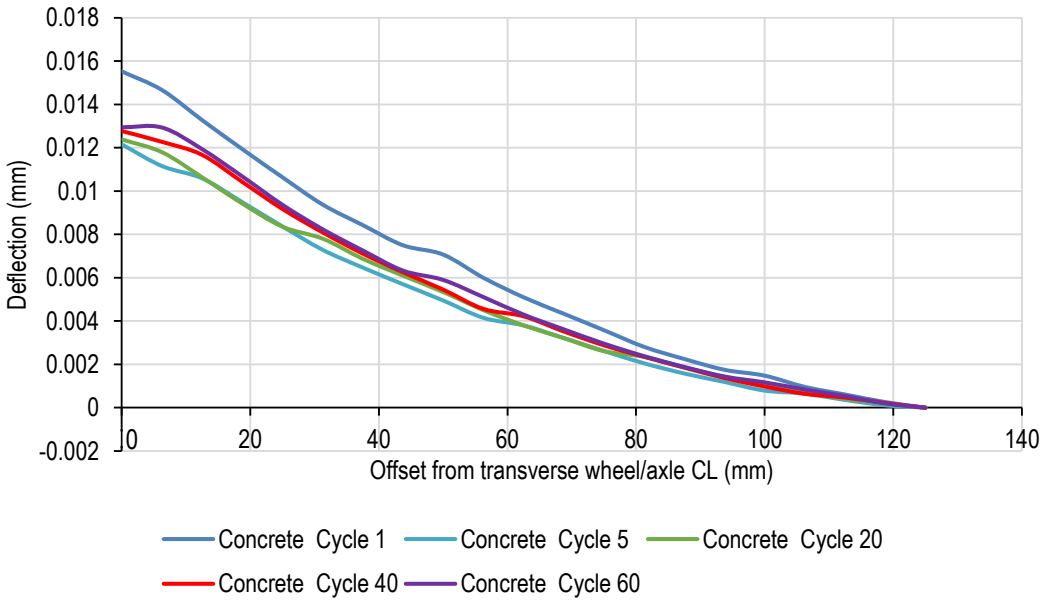

Figure 14 Change of concrete layer deflection bowls with load cycles relative to the point at rest before loading

The deflection bowl for the stabilized base layer for different wheel load cycle can be seen in Figure 15. The bowls indicate that significant damage took place with the first load cycle and virtually no deflection was recorded in any subsequent load cycles. The change in the width of the deflection bowl should be noted. During the first load cycle, the base layer started deflecting in the wheel path due to the approaching wheel load, when the load was still more than 120 mm from the measurement point. This is the same distance than for the concrete surface layer, which would make sense for a bonded layer system. After the first load cycle, the base layer deflection bowl width decreased to about 50mm, which means that the base layer did not deflect at all, while the concrete layer started deflecting under the wheel load, up to the point where nearly 50% of the concrete deflection had taken place.

These results indicate that there is no real bond between the concrete surface and the base layer. After the permanent deformation of the base layer in the wheel path, caused by the first wheel load cycle, no contact existed and thereafter the concrete had to carry

the wheel load unsupported until the concrete layer under the wheel load deflected sufficiently to make contact with the rutted base layer. The steel reinforcing in the width of the thin concrete layer must thus be sufficient to prevent cracks from opening up while the thin concrete layer spans over the width of the rutted wheel path in the base layer.

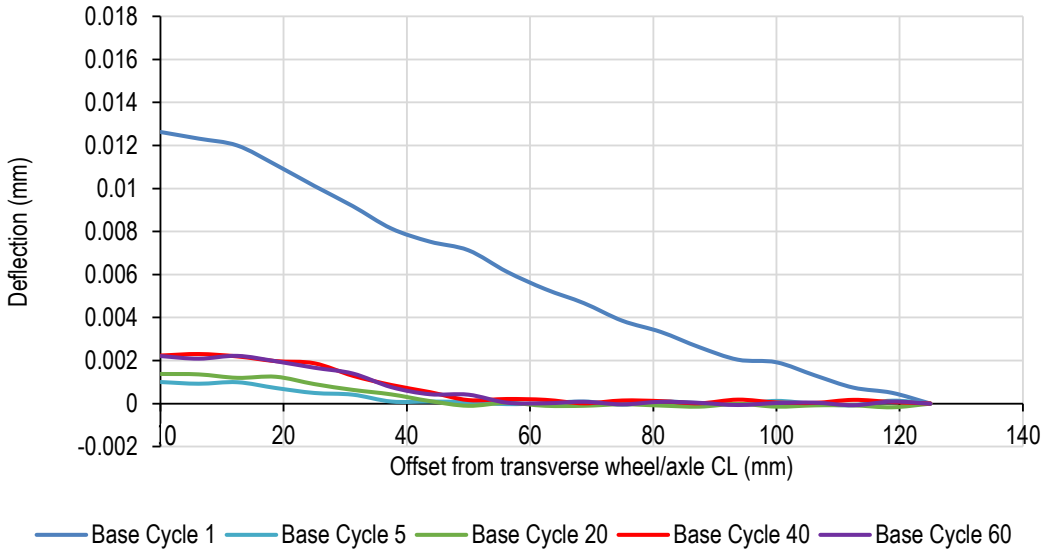

Figure 15 Change of base layer deflection bowls with load cycles relative to the point at rest before loading

Vertical displacement distribution

The loaded and unloaded vertical displacement at depth measured for selected applied load cycles are shown in Figure 16. The vertical displacement distributions (VDD) in the wheel CL are shown in Figure 16 (a) and VDD in the axle CL are shown in Figure 16 (b). Note that the scale of the x-axis of Figure 16 (a) is different than that of Figure 16 (b). The solid lines indicate the Loaded (L) distributions while the dashed lines indicate the Unloaded (UL) distributions.

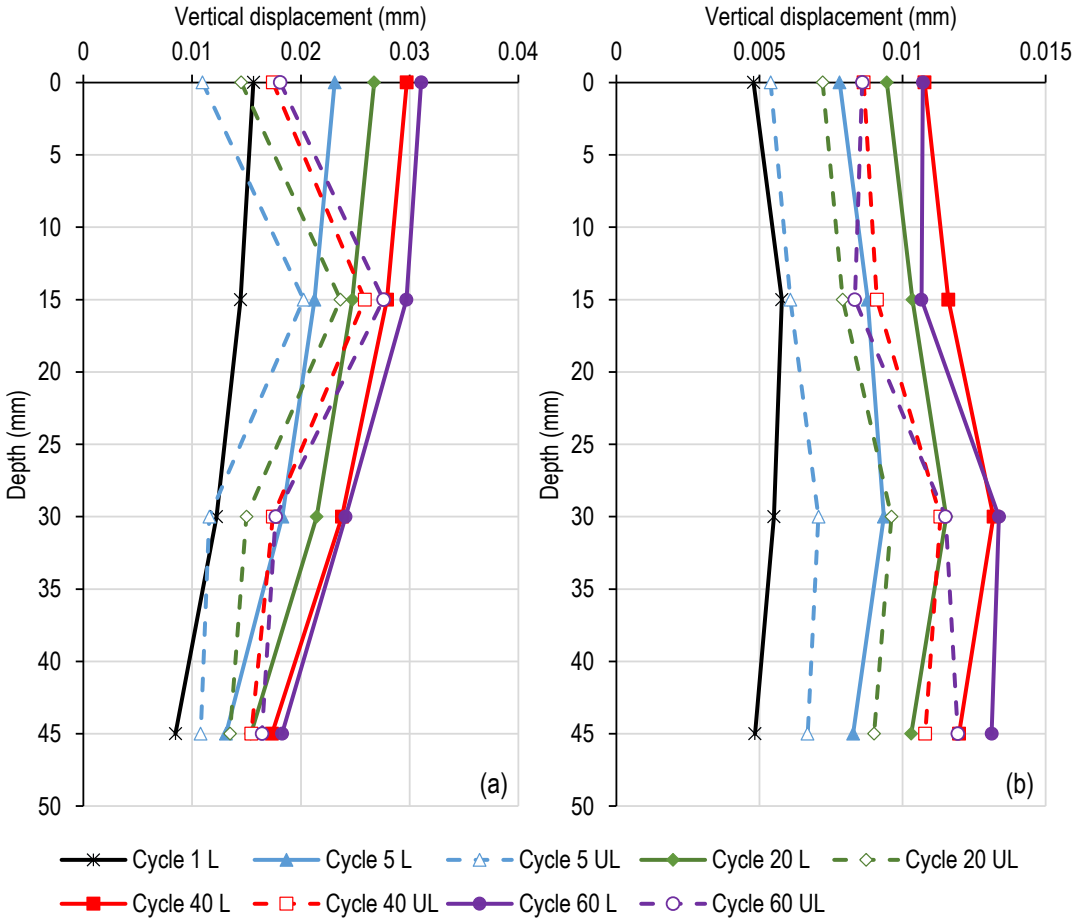

Figure 16 Loaded and unloaded VDD in (a) wheel CL and (b) axle CL

As expected the maximum deflection took place on the surface in the wheel path. With every load cycle the deflection under the wheel increased notably, but the rate of increase decreased with number of load cycles and between cycle 40 and 60 there was only a marginal increase in deflection under load. The same can be said for the permanent displacement. This indicates that the pavement reached a resilient state where the condition of the pavement should remain constant for a large number of load cycles.

Looking at the difference in deflection between the loaded and unloaded condition of each layer, the cemented base layer behaves differently from the other layers. Both the concrete layer, above the cemented base layer, and the subbase below the stabilized base

layer, show substantial deflection recovery when the load moved away from the measurement point. In contrast the cemented base layer deflected notably under load, but showed very little deflection recovery when the load was removed. As the concrete layer cannot consolidate or compact under the wheel load, these results indicate that a gap formed between the concrete surface layer and the supporting stabilized layer, leaving the unsupported concrete surface layer to span over the rut formed under the concrete as a result of the permanently deformed base layer. The lack of elastic behaviour of the stabilized base layer, indicates that this layer sustained permanent damage in the wheel path, such as cracking, during the first load cycles.

The vertical displacement under the axle centreline between the wheel paths shows interesting behaviour, with the supporting layers displacing more than the concrete surface layer under both loaded and unloaded conditions. This again indicates that a gap probably formed between the concrete layer and the supporting soil layers. With the relatively small deformations under the axle centreline, the cemented base layer seems undamaged and all layers show increased deformation with increase in number of load cycles for both the loaded and un-loaded conditions. The rate of increase in deformation decreased with number of load cycles, again indicating resilient behaviour.

Discussion

The results of the current investigation confirm the trends observed by Smit and Kearsley (2022). The reduced model depth and increased layer stiffness reduced the measured deformation notably. The advantage of the sand-based centrifuge scale models used in the earlier study was that the exaggerated deformations provided a clear qualitative representation of the behaviour of a thin, ductile concrete layer under moving axle loads. The qualitative model moved the focus of the research from only studying the behaviour in the wheel paths to taking the whole cross section of the pavement into account.

Based on the results of this investigation it is clear that the UTCRCP can be designed as neither a rigid nor a flexible pavement. A rigid pavement would have no differential movement over the cross section of the pavement, while the vertical displacement of a flexible pavement would have been confined to the loaded area in the supporting layers, not having any effect on the top of the pavement at the centre of the axle.

It can thus be hypothesised that the UTCRCP surface layer acts as a membrane, confining the material supporting the concrete layer. When the base layer in the wheel path deforms, the concrete layer moves down and places downward pressure on the material adjacent to the wheel path. The supporting layers are placed in compression under the wheel paths and the material moves towards the centre of the axle, resulting in upward pressure placed on the concrete surface layer between the wheel paths. This upwards pressure causes upward bending (or hogging) and can result in longitudinal cracks forming and opening between the wheel paths if insufficient transverse reinforcing is placed in the concrete surface layer. In the wheel path the concrete surface layer needs to bridge the gap that forms below it when the base layer is permanently deformed by the first wheel loads that pass over the pavement.

The damage to the base layer should not have any negative effect on the lifespan of the pavement, on condition that sufficient reinforcing is placed in the concrete layer, to ensure ductile behaviour under repeated wheel load cycles. The UTCRCP can thus only operated effectively if the surface layer is thin enough to behave as a membrane, with a layer of reinforcing placed in the centre of the depth of the concrete layer to ensure that the steel reinforcing can handle the tensile forces caused both under the wheel loads and below the centre of the axle, between the wheel loads.

Conclusions & recommendations

Based on the experimental results it can be concluded that:

- Scaling of unstabilised layerworks results in lack of confinement causing reduced stiffness, possibly affecting behaviour under load cycles.
- Centrifugal forces can be used to ensure realistic soil behaviour in scaled pavement models.
- Plate bearing tests results indicated that it was possible to construct a layered system with only scaled granular layers failing in a ductile manner with increasing stiffness as the compaction effect increased, but also having scaled stabilized layers being stiff and brittle.
- The results obtained from single wheel HVS testing of UTCRCP may not model the actual behaviour and failure mechanism of UTCRCP exposed to repeated rolling axle loads.
- UTCRCP cannot be designed as a rigid or a flexible pavement
- UTCRCP must be designed taking possible rutting of support layers into account.
- UTCRCP must be designed for the upward bending, or hogging, that could take place between the wheel paths.
- Layers supporting highly reinforced thin concrete surface layers must be designed considering the ductile behaviour of the concrete layer.

Although the use of UTCRCP is promising further research should be conducted to find the most suitable design assumptions for layerworks supporting UTCRCP surface layers. The optimal strength, thickness and reinforcing content for the thin concrete surface layer, in combination with suitable support conditions, must be established to ensure that UTCRCP can live up to expectations.

References

ARA, I. and Division, E.C., 2004. *Guide for Mechanistic-Empirical Design of New and Rehabilitated Pavement Structures, NCHRP 1-37A Final Report*. Washington, D.C.

Bayton, S.M., Elmrom, T., and Black, J.A., 2018. Centrifuge modelling utility pipe behaviour subject to vehicular loading. *In*: *Physical Modelling in Geotechnics*. 163–168.

Bowles, J.E., 1996. *Foundation analysis and design*. 5th ed. New York: McGraww-Hill.

Bowman, A.J. and Haigh, S.K., 2019. Subsurface deformation mechanisms beneath a flexible pavement using image correlation. *Geotechnique*, 69 (7), 627–637.

Bueno, M., Arraigada, M., and Partl, M.N., 2016. Damage detection and artificial healing of asphalt concrete after trafficking with a load simulator. *Mechanics of Time-Dependent Materials*, 20 (3), 265–279.

Dave, T.N. and Dasaka, S.M., 2018. Experimental model study on traffic loading induced earth pressure reduction using EPS geofoam. *In*: *Physical Modelling in Geotechnics*. 169–174.

Denneman, E., 2011. Fracture in High Performance Fibre Reinforced Concrete Pavement Materials. University of Pretoria.

Gerber, J.A.K., 2011. Charaterization of cracks on Ultra-Thin Continuously REinforced Concrete Pavements. Stellenbosch University.

Huang, Y.H., 1993. *Pavement Analysis and Design*. 2nd ed. New Jersey: Pearson Prentice Hall.

Kannemeyer, L., Perrie, B.D., Strauss, P.J., and Du Plessis, L., 2007. Ultra-Thin Continuously Reinforced Concrete Pavement research in South Africa. *In*: *International Conference on Concrete Roads*. 97–124.

Kearsley, E.P., Steyn, W.J. vdM., and Jacobsz, S.W., 2014. Centrifuge modelling of Ultra Thin Continuously Reinforced Concrete Pavements (UTCRCP). *In*: *International Conference on Physical Modelling in Geotechnics*. 1101–1106.

Lukiantchuki, J., Oliveira, J.R.M.S., Pessin, J., and Almeida, M., 2018. Centrifuge modelling of traffic simulation on a construction waste layer. *International Journal of Physical Modelling in Geotechnics*, 18 (6), 290–300.

Marais, L.R. and Perrie, B.D., 1993. *Concrete industrial floors on the ground*. 1st ed. Midrand, South Africa: Cement & Concrete Institute.

Martin, A.E., Walubita, L.F., Hugo, F., and Bangera, N.U., 2003. Pavement response and rutting for full-scale and scaled APT. *Journal of Transportation Engineering*, 129 (4), 451–461.

Mones Ruiz, H.A., Grabe, P.J., and Maina, J.W., 2019. A mechanistic-empirical method for the characterisation of railway track formation. *Transportation Geotechnics*, 18 (October 2018), 10–24.

Saboya, F., Tibana, S., Martins Reis, R., Durand Farfan, A., and Maria de Assis Rangel Melo, C., 2020. Centrifuge and Numerical Modeling of Moving Traffic Surface Loads on Pipelines Buried in Cohesionless Soil. *Transportation Geotechnics*, 23 (October 2019), 100340.

Smit, M.S. and Kearsley, E.P., 2022. Centrifuge modelling of Ultra-Thin High Strength

Steel Fibre Reinforced Concrete Pavements. *International Journal of Physical Modelling in Geotechnics*, (8.5.2017), 2003–2005.

Van de Ven, M.F.C. and De Fortier Smit, A., 2000. The role of the MMLS devices in APT. *In*: *Proceeding of the Southern African Transport Conference*. Pretoria, South Africa: SATC.

Westergaard, H.M., 1926. Stresses in concrete pavements computed by theoretic analysis. *Public Roads*, 7 (2), 25–35.